

Oscillating axion bubbles as alternative to supermassive black holes at galactic centers

Anatoly A. Svidzinsky

Department of Physics, Institute for Quantum Studies,
Texas A&M University, College Station, TX 77843-4242

asvid@jewel.tamu.edu

(Dated: July 25, 2018)

Recent observations of near-infrared and X-ray flares from Sagittarius A*, which is believed to be a supermassive black hole at the Galactic center, show that the source exhibits about 20-minute periodic variability. Here we provide arguments based on a quantitative analysis that supermassive objects at galactic centers may be bubbles of dark matter axions rather than black holes. An oscillating axion bubble can explain periodic variability of Sagittarius A* and yields the axion mass about 0.6 meV which fits in the open axion mass window. The bubble scenario with no other free parameters explains lack of supermassive “black holes” with mass $M < 10^6 M_\odot$. Low-mass bubbles decay fast and as a result are very rare. We also found that the mass of an axion bubble can not exceed $1.5 \times 10^9 M_\odot$, in agreement with the upper limit on the supermassive “black hole” mass obtained from observations. Our finding, if confirmed, suggests that Einstein general relativity is invalid for strong gravity and the gravitational field for the bubble effectively becomes repulsive at large potential. Imaging a shadow of the “black hole” at the Galactic center with VLBI in the next decade can distinguish between the black hole and the oscillating axion bubble scenarios. In the case of axion bubble, a steady shadow will not be observed. Instead, the shadow will appear and disappear periodically with a period of about 20 min.

I. INTRODUCTION

Originally introduced to explain why the strong interaction, in contrast to weak interactions, does not violate CP symmetry [1], hypothetical axions have since become one of the leading particle candidates for the cold dark matter in the Universe [2]. The axion appears as a pseudo Nambu-Goldstone boson of a spontaneously broken Peccei-Quinn symmetry [1], whose scale f determines the axion mass m ,

$$m \approx \frac{m_\pi f_\pi}{2f} = 0.62 \text{ eV} \cdot \frac{10^7 \text{ GeV}}{f} \quad (1)$$

and suppresses the coupling to Standard Model particles, $\propto 1/f$. Here $m_\pi = 135$ MeV is the neutral pion mass and $f_\pi = 93$ MeV its decay constant [2, 3]. Astrophysical and cosmological arguments constrain the axion mass m to be in the range of $10^{-6} - 3 \times 10^{-3}$ eV [2]. Axions in this mass range could provide much or all of the cold dark matter in the Universe. Properties of stars impose the upper limit on the axion mass via constraints on axion interaction with photons, leptons and nucleons. However, such interactions are model-dependent. Observations of the cosmological large-scale structure constrain the axion-pion coupling which yield weaker upper mass limit $m < 1.05$ eV [4].

Interaction of axions with QCD instantons generates the axion mass and periodic interaction potential [5]

$$V(\varphi) = m^2 f^2 [1 - \cos(\varphi/f)], \quad (2)$$

where φ is a real scalar axion field.

Here we argue that oscillating axion bubbles, rather than supermassive black holes, could be present at galactic centers. Recent observations of near-infrared and X-ray flares from Sagittarius A*, which is believed to be

a $3.6 \times 10^6 M_\odot$ black hole at the Galactic center, show that the source exhibits about 20-minute periodic variability [6, 7, 8]. An oscillating axion bubble can explain periodic variability of Sagittarius A* and yields the axion mass about 0.6 meV. Fig. 1 explains the mechanism of flare variability.

Moreover, the bubble scenario explains observed lack of supermassive “black holes” with mass $M < 10^6 M_\odot$. As we discuss later in this paper the bubble life-time $t \propto M^{9/2}$, it becomes less than the age of the Universe for $M \lesssim 5 \times 10^6 M_\odot$. The bubble at our Galactic center would decay within about 5×10^9 yrs. If, however, $M < 10^6 M_\odot$ the decay time becomes very short, $t \lesssim 10^7$ yrs, and as a result such objects are very rare.

Finally, the axion bubbles with no free parameters (if we fix $m = 0.6$ meV based on Sagittarius A* flare variability) explain the upper limit ($1.5 \times 10^9 M_\odot$) on the supermassive “black hole” mass found in recent analysis of the measured mass distribution [9].

In recent years, the evidence for the existence of an ultra-compact concentration of dark mass associated with the radio source Sagittarius A* in the Galactic Center has become very strong. However, an unambiguous proof that this object is a black hole is still lacking. A defining characteristic of a black hole is the event horizon. To a distant observer, the event horizon casts a relatively large “shadow” with an apparent diameter of about 10 gravitational radii due to bending of light. The predicted size (~ 30 micro-arcseconds) of this shadow for Sagittarius A* approaches the resolution of current radio-interferometers. Hence, there exists a realistic expectation of imaging the shadow of a black hole with very long-baseline interferometry within the next decade [10, 11, 12, 13]. Such imaging will allow us to distinguish between the black hole and the oscillating axion bubble

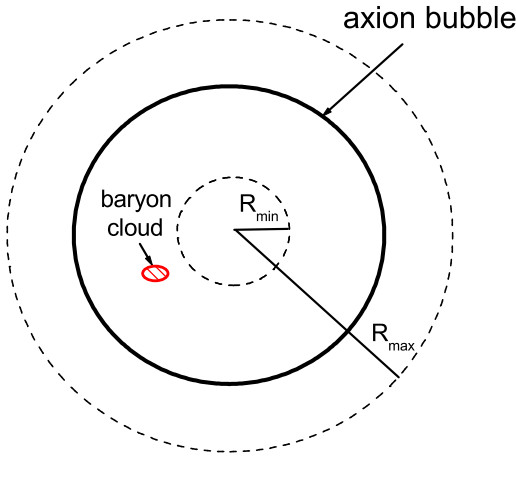


FIG. 1: Mechanism of flare variability. Axion bubble radius oscillates between R_{\min} and R_{\max} which yields periodic variation of the gravitational redshift $z(t)$ of the bubble interior. The dark matter bubble itself does not radiate electromagnetic waves; radiation is produced by flaring clouds of baryon matter trapped in the bubble interior. Redshift $z(t)$ reduces radiation power of the cloud by a factor of $1/(1+z(t))^2$. As a result, intensity of the flaring cloud radiation is modulated with the period of bubble oscillation. Modulation amplitude depends on the distance between the cloud and the bubble center.

scenario which we propose in this paper. If the axion bubble, rather than a black hole, is present at the Galactic center, the steady shadow will not be observed. Instead, the shadow will appear and disappear periodically with a period of about 20 min.

II. AXION BUBBLES

We introduce dimensionless coordinates and define the unit of distance, time and φ as

$$r_0 = \frac{\hbar}{mc}, \quad t_0 = \frac{\hbar}{mc^2}, \quad \varphi_0 = \frac{1}{\sqrt{4\pi G}}, \quad (3)$$

where c is the speed of light and G is the gravitational constant. For the moment we omit gravity. Further we use natural units for which $\hbar = c = 1$. Energy of the axion field in units of m_{pl}^2/m is given by

$$E = \int d\mathbf{r} \left[\frac{1}{2} \left(\frac{\partial \varphi}{\partial t} \right)^2 + \frac{1}{2} (\nabla \varphi)^2 + V(\varphi) \right], \quad (4)$$

where

$$V(\varphi) = \frac{1}{\alpha^2} [1 - \cos(\alpha\varphi)], \quad \alpha = \frac{1}{\sqrt{4\pi G f}} = \frac{m_{\text{pl}}}{\sqrt{4\pi f}} \quad (5)$$

is the dimensionless potential and the coupling parameter respectively, $m_{\text{pl}} = \sqrt{\hbar c/G} = 1.2 \times 10^{19}$ GeV is the Planck mass.

The interaction potential V has degenerate minima $V = 0$ at $\varphi = 2\pi n/\alpha$, where n is an integer number. As a consequence, equation for the axion field φ has bubble-like solutions. The bubble surface is an interface between two degenerate vacuum states with $\varphi = 2\pi n/\alpha$ ($r < R$) and $\varphi = 0$ ($r > R$). In this paper we consider spherical bubbles with surface width much smaller than its radius R and $n = 1$. Energy density of the axion field is nonzero only at the bubble surface. Energy of a static thin-wall bubble is $E = 4\pi\sigma R^2$, where σ is the surface energy per unit area (which equals to the surface tension for the domain wall we consider [14]) determined by an integral over one potential period [15, 16]

$$\sigma = \frac{1}{4\pi} \int \sqrt{2V} d\varphi = \frac{2}{\pi\alpha^2}. \quad (6)$$

Surface tension σ depends only on the axion interaction strength. The later, however, slightly depends on the axion model which can change Eq. (6) by a factor of the order of one [17].

Under the influence of surface tension an initially static bubble collapses to its center which yields reduction of the surface energy. However, if we include gravity this gives an additional energy contribution. Such a contribution could substantially alter the bubble evolution and, in particular, prevent collapse as we discuss in the next section.

One should mention that decay of axions into photons is suppressed in the bubble. Such a decay is not allowed by energy conservation. The bubble surface is approximately a one dimensional kink. In the kink's reference frame the kink is static and the distribution of the axion field is obtained by minimization of the energy functional (4) subject to the boundary conditions that far from the kink we have fixed vacuum states ($\varphi = 0$ from one side and $\varphi = 2\pi/\alpha$ from the opposite side). The optimized field distribution determines the kink's energy. Any small change in φ would increase the total energy of the axion field. Axions in the kink cannot decay into photons because annihilation of the axion would change the distribution of the axion field in the kink and, hence, increase the kink's energy. In such a process both the axion field and photon acquire energy which violates energy conservation.

III. THE ALTERNATIVE THEORY OF GRAVITY VS EINSTEIN GENERAL RELATIVITY

So far Einstein general relativity has successfully passed all available tests. However such tests have inspected the theory only at weak gravitational field [18]. One should note that observations of binary pulsars yet have not provided a test of general relativity at

strong gravity. Rather, such observations tested Einstein equations in the post-Newtonian approximation and the strong equivalence principle [18].

Are Einstein equations valid for strong gravity? The answer to this question remains unknown and only appropriate observational tests can shed light on it. It is well known that in Einstein general relativity the gravitational field disobeys the principle of superposition. This is the consequence of the postulate that the space-time metric is determined by the Einstein equations

$$R_{ik} - \frac{1}{2}g_{ik}R = 8\pi T_{ik}, \quad (7)$$

with the particular choice of the matter energy-momentum tensor T_{ik} proposed by Einstein. However the Einstein theory can be modified by modifying the energy-momentum tensor. This yields a possibility to satisfy the superposition principle by a proper choice of T_{ik} .

In Appendix A we derive a space-time metric produced by a static mass distribution based only on the superposition principle. The answer is given by the Yilmaz exponential metric. Then we show that the Einstein equations yield the exponential metric if T_{ik} is taken as an “electrostatic” energy-momentum tensor.

In the weak field limit the exponential metric is equivalent to those obtained in Einstein theory and, hence, the exponential metric agrees with the four classic tests of general relativity. However in the opposite limit of strong gravity the exponential metric is dramatically different. Since the superposition principle is satisfied the exponential metric predicts no black holes, but rather stable compact objects with no event horizon and very large, but finite, gravitational redshift (“dark red holes”). This suggests that gravitational field for those objects effectively becomes repulsive at large gravitational potential.

Here we analyze properties of compact objects at galactic centers and show that they are in favour of the exponential metric. Our conclusion is based on a quantitative analysis which is independent of the particular choice of the time-dependent theory of gravity [19]. This is possible because the main part of the bubble dynamics we use for the quantitative comparison occurs in the well-tested limit of Newtonian gravity. Only a small part of the trajectory near the lower radius turning point (where gravity effectively becomes repulsive) is beyond Newtonian description. As a result, e.g., the period of bubble oscillation can be accurately obtained using Newtonian gravity, independent of which theory of gravity yields the repulsive force at small radius.

A. Bubbles in exponential metric

In Appendix A we derive a metric for a static mass distribution assuming that the gravitational field obeys the principle of superposition for any field strength. The

answer is given by an exponential isotropic line element of the class proposed by Yilmaz [20, 21]

$$ds^2 = -e^{2\phi}dt^2 + e^{-2\phi}(dx^2 + dy^2 + dz^2), \quad (8)$$

where for a spherically symmetric thin-wall bubble of radius R (units are $c = G = 1$)

$$\phi(r) = \begin{cases} -M/r, & r \geq R \\ -M/R, & r < R, \end{cases} \quad (9)$$

and M is the bubble mass. The exponential metric does not have the singularity of the Schwarzschild solution at finite radius, and therefore replaces the concept of black holes with that of “dark red holes”.

In the reference frame of a distant observer the energy of a static bubble is given by [22]

$$U(R) = 4\pi\sigma R^2 \exp\left(\frac{M}{R}\right), \quad (10)$$

where σ is the intrinsic surface energy density (as it would appear to an observer located at the bubble surface) given by Eq. (6), M is the dimensionless bubble mass in units of m_{pl}^2/m and R is the dimensionless bubble radius in units of r_0 . If the radius of a spherical bubble changes with time then the total energy is

$$E = U(R) + E_k, \quad (11)$$

where $E_k \geq 0$ is the kinetic energy. The total energy E is a constant of motion, then based on the equivalence principle we obtain $M = E = \text{const}$. Evolution of the bubble radius is similar to a one dimensional motion of a particle in the effective potential $U(R)$. We plot $U(R)$ in Fig. 2. The effective potential has a shape of a well and depends on the total energy (mass). At $R \gg M$ one can omit gravity and $U(R) \simeq 4\pi\sigma R^2$ is just a surface energy (tension) which tends to contract the bubble. At $R \ll M$ gravity produces large repulsive effective potential which forces the bubble to expand. As a result the bubble radius $R(t)$ oscillates between two turning points determined by $U(R) = M$.

Fig. 3 shows numerical solution of the equation for turning points $M = 4\pi\sigma R^2 \exp(M/R)$. For $4\pi\sigma M < 4/e^2 = 0.541$ equation has two solutions; radius of such bubbles oscillates with time between turning points R_1 and R_0 . If $M = M_{\text{max}} = 1/(e^2\pi\sigma)$ the bubble is static with $R = M/2$. Such static bubble possesses maximum possible mass. Bubbles with $M > M_{\text{max}}$ do not exist. As we show below, for the Galactic center bubble $M \ll M_{\text{max}}$.

In a general case to describe $R(t)$ quantitatively we need to use dynamic equations. These equations depend on a particular choice of the time-dependent theory of gravity. In this paper, however, we do not need them which makes our results quite general. The point is that if the Galactic center object is an axion bubble the main part of its periodic oscillation occurs in the limit $R(t) \gg M_{\text{max}}$.

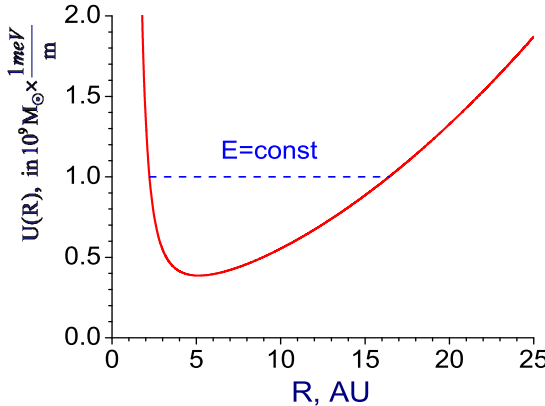


FIG. 2: Effective potential for axion bubble motion $U(R)$ (solid line) in Yilmaz exponential metric. Bubble radius $R(t)$ oscillates between turning points determined by the equation $U(R) = E$. We expressed R in Astronomical Units (AU) and $U(R)$ in solar masses, m is the axion mass.

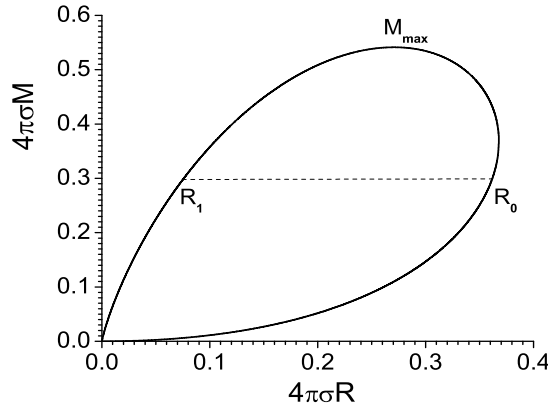


FIG. 3: Mass-radius relation for a bubble in Yilmaz exponential metric. At a given mass M the bubble radius $R(t)$ oscillates between turning points R_1 and R_0 . If $M = M_{max}$ then $R_1 = R_0$ and the bubble is static.

M . In this region we can omit gravity and use the well-tested special theory of relativity that yields the following mass-radius equation for a relativistic bubble

$$M = \frac{4\pi\sigma R^2}{\sqrt{1 - (dR/dt)^2}} \quad (12)$$

which has a simple solution

$$R(t) = R_0 \operatorname{cn} \left(\frac{\sqrt{2}t}{R_0}, \frac{1}{\sqrt{2}} \right), \quad (13)$$

where $R_0 = \sqrt{M/4\pi\sigma}$ is the maximum bubble radius and

$\operatorname{cn}(x, k)$ is Jacobian elliptic cosine. For small $R(t)$ the solution (13) is not applicable. In this region the bubble shrinking slows down and after reaching the inner turning point R_1 the bubble starts to expand. Assuming that Eq. (13) is accurate for the main part of the motion we obtain that the period of bubble oscillation is $T \simeq 2.622R_0$. Taking into account that $M = 4\pi\sigma R_0^2 = 8R_0^2/\alpha^2$, we get in dimension units $T \simeq 0.262\sqrt{M/m\hbar}/fc^2$. Then using Eq. (1) we find

$$T \simeq 0.523 \frac{\hbar \sqrt{Mm}}{c^2 m_\pi f_\pi} = \sqrt{\frac{M}{10^6 M_\odot} \frac{m}{10^{-3} \text{eV}}} \times 15.27 \text{ min.} \quad (14)$$

If $M = 3.6 \times 10^6 M_\odot$ and $T = 22.2$ min [8] then Eq. (14) yields the axion mass $m \simeq 0.6$ meV ($f \simeq 10^{10}$ GeV). One should mention, however, that due to time dilation the period of flare variability depends on the distance between the flare source and the bubble center (see Fig. 1) and, thus, could differ from Eq. (14) by a factor of the order of one. This yields an inaccuracy in the axion mass determination in the same factor.

Next we discuss the bubble life time. The bubble decay occurs by means of axion emission. Due to spherical symmetry there is no radiation of gravitational waves. Bubble surface, the interface between different vacuum states, is a soliton (or a kink) that is studied in many areas of nonlinear physics. One dimension solitons, contrary to 2D or 3D, are stable and preserve their shape under reflection from a boundary. Because a thin-wall bubble surface can be treated as a 1D soliton this insures its very long life time. However, due to finite bubble radius the 1D treatment is only approximate. Deviation of the problem from 1D leads to slow decay of the soliton by emission of particles (axions).

We estimate the bubble decay rate as the time of energy loss by the bubble with the radius $R(t)$ oscillating between the outer R_0 and inner R_1 turning points. Energy loss by the bubble surface becomes substantial only when $R(t) \lesssim R_0^{2/3}$ (see Appendix B below). In our case $R_1 \gg R_0^{2/3}$ and, therefore, the region of intensive energy dissipation is not accessible. As a result, the energy emission is negligible yielding long-lived bubbles. In Appendix B we estimate the bubble life-time. The answer is given by Eq. (B11) which in dimension units reads

$$t \sim \frac{R_0}{c} \left(\frac{R_1}{R_0} \right)^4 \left(\frac{R_1}{r_0} \right)^2. \quad (15)$$

If $m = 0.6$ meV then the bubble surface has thickness $r_0 = \hbar/mc = 0.3$ mm. For a bubble with mass $M = 3.6 \times 10^6 M_\odot$ the maximum radius is $R_0 = 483 R_\odot$, while the gravitational radius $R_g = 16.1 R_\odot$. One can find the inner turning point R_1 from the equation $R_0^2 = R_1^2 \exp(M/R_1)$ which yields $R_1 = 1.1 R_\odot$. Using Eq. (15) we then obtain the bubble life time $t \sim 5 \times 10^9$ yrs. This can explain observed lack of supermassive “black holes” with $M < 10^6 M_\odot$. Axion bubbles with such masses decay fast with life time $t \propto M^{9/2}$.

For bubbles with $M \ll M_{\max}$ one can obtain R_1 in terms of the bubble mass M analytically

$$R_1 = \frac{M}{2 \ln \left[\frac{2R_0}{M} \ln \left(\frac{2R_0}{M} \right) \right]}, \quad R_0 = \alpha \sqrt{\frac{M}{8}}. \quad (16)$$

Substitute this into Eq. (15) yields the following expression for the bubble life-time

$$\begin{aligned} t &\sim \frac{\pi^{3/2} \hbar m_{\pi}^3 f_{\pi}^3 \sqrt{m} M^{9/2}}{\sqrt{8} c^2 m_{\text{pl}}^{12} \ln^6 [x \ln(x)]} = \\ &= \left(\frac{M}{10^6 M_{\odot}} \right)^{9/2} \sqrt{\frac{m}{10^{-3} \text{eV}}} \times \frac{4.73 \times 10^{11}}{\ln^6 [x \ln(x)]} \text{ years}, \quad (17) \end{aligned}$$

where

$$x = \frac{m_{\text{pl}}^2 \sqrt{m}}{\sqrt{2\pi} m_{\pi} f_{\pi} \sqrt{M}} = 140 \sqrt{\frac{m}{10^{-3} \text{eV}}} \frac{10^6 M_{\odot}}{M}.$$

Eq. (17) shows that the bubble life-time $t \propto M^{9/2}$ and it becomes less than the age of the Universe for $M \lesssim 5 \times 10^6 M_{\odot}$. For $M < 10^6 M_{\odot}$ the decay time becomes very short, $t \lesssim 10^7$ yrs, this is why we do not observe supermassive “black holes” with such masses.

Recent analysis of the mass distribution for the compact objects at galactic centers shows existence of an upper limit for the supermassive “black hole” mass [9]:

$$M_{\max} = 1.2^{+2.6}_{-0.4} \times 10^9 M_{\odot}. \quad (18)$$

Next we calculate the maximum possible mass of an axion bubble. In dimension units it is given by

$$M_{\max} = \frac{0.0215 m_{\text{pl}}^4 m}{m_{\pi}^2 f_{\pi}^2}. \quad (19)$$

For $m = 0.6 \text{ meV}$ Eq. (19) yields $M_{\max} = 1.5 \times 10^9 M_{\odot}$. This value agrees with the upper limit on the supermassive “black hole” mass (18) measured for galactic nuclei. Radius of the static bubble with M_{\max} is $R = 1673 R_{\odot}$.

B. Bubble in Einstein general relativity

In Einstein general relativity for a spherically symmetric bubble the metric can be written in the form

$$ds^2 = -h dt^2 + g dr^2 + r^2 d\Omega^2, \quad (20)$$

where g , the radial metric, and h , the lapse, are functions of t and r with r being the circumferential radius. For a static thin-wall bubble of radius R the Einstein equations yield

$$h(r) = \begin{cases} 1 - 2M/r, & r \geq R \\ 1 - 2M/R, & r < R, \end{cases} \quad (21)$$

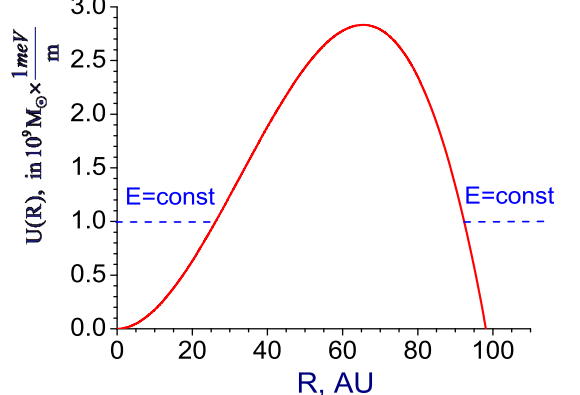


FIG. 4: Effective potential for axion bubble motion in Einstein general relativity. “Small” bubbles shrink to black holes, while large bubbles expand infinitely. We expressed R in Astronomical Units (AU) and $U(R)$ in solar masses.

$$g(r) = \begin{cases} \frac{1}{1-2M/r}, & r > R \\ 1, & r < R. \end{cases} \quad (22)$$

Note that $g(r)$ undergoes a jump at the bubble surface, while exponential metric (8), (9) is continuous. Energy of the thin-wall bubble with radius $R(t)$ is given by [23, 24]

$$E = \frac{4\pi\sigma R^2}{\sqrt{1 - (dR/d\tau)^2}} - 8\pi^2\sigma^2 R^3, \quad (23)$$

where τ is the interior coordinate time ($d\tau^2 = h dt^2$). The corresponding effective potential

$$U(R) = 4\pi\sigma R^2 - 8\pi^2\sigma^2 R^3 \quad (24)$$

is pictured in Fig. 4.

In Einstein theory “small” bubbles shrink toward the gravitation radius $R_g = 2M$ and at $t \gg R_g/c$ behave as black holes, while large bubbles expand infinitely. This is dramatically different from bubble evolution in the exponential metric which we discussed in the previous section. At the same time, the exponential and the isotropic form of the Schwarzschild metric (A2) are the same to second order in the gravitational potential ϕ in the temporal part and to first order in the spatial part (see Appendix A). This is sufficient to insure that they both give identical results in the four classic weak-field tests of general relativity.

IV. DISCUSSION

If axion bubbles, rather than supermassive black holes, are located at galactic centers then what is the mechanism of their nucleation? Dark matter axions, if they exist, form halos around galaxies. The halo of axions is

in a quantum degenerate non-equilibrium regime. Evolution of the axion halo is governed by the self-gravity and axion interaction $V(\varphi)$. The interaction $V(\varphi)$ becomes important only for dense axion clumps. Dynamics of a dilute galactic halo is determined by self-gravity. Seidel and Suen have studied evolution of a massive, self-gravitating real scalar field in Newtonian limit (omitting self-interaction $V(\varphi)$) [25]. They have shown that independent of the initial conditions a scalar field configuration collapses to form a compact object by ejecting part of the scalar field, carrying out the excess kinetic energy. The cooling occurs due to nonlinear effects of the self-gravitation of the field. Characteristic cooling time is a free falling time to the center due to self gravity $t \simeq 2R_{\text{halo}}^{3/2}/\sqrt{2GM_{\text{halo}}}$, where R_{halo} and M_{halo} is an initial radius and mass of the axion halo in a galaxy. For $R_{\text{halo}} = 60$ kpc and $M_{\text{halo}} = 10^{12}M_{\odot}$ we obtain the characteristic cooling time $t \sim 10^8$ yrs.

Thus, within about 10^8 yrs the gravitational cooling mechanism yields formation of compact axion clumps in a galactic halo. Evolution of such clumps is then governed by self-interaction $V(\varphi)$ which leads to bubble formation. This is shown by three-dimensional numerical simulation of the evolution of inhomogeneities in the axion field due to the self-interaction $V(\varphi)$ [26]. Such a simulation (which omits gravity) has indeed demonstrated formation of bubble-like structures (see Fig. 5a in Ref. [26]). The mass of the nucleated bubbles is much smaller than the mass of the halo they are born in. However for typical halos many bubbles are born with masses much greater than 10^6M_{\odot} and hence they are long-lived objects.

In Einstein general relativity axion bubbles under the influence of surface tension collapse fast into black holes. However, the Einstein theory yet to be tested in the limit of strong gravitational field. There is a possibility that at strong field the gravity is not described by Einstein general relativity, and rather by an alternative theory which also passes all available tests. In this paper we consider axion bubbles in a very general approach avoiding a particular choice of the alternative time-dependent theory of gravity. Our results are valid for any metric theory which is based on the principle of superposition. This principle yields the exponential metric in the static limit, as shown in Appendix A. One should mention that if the space-time geometry is described by the exponential metric then compact supermassive objects at galactic centers can not be made of baryonic matter. Maximum mass of a compact (neutron star like) baryonic object in such a metric can not exceed about $12M_{\odot}$ [27]. Hence, dark matter of non baryonic origin is the only alternative for their composition.

We found that in the exponential metric the axion bubbles with $M > 10^6M_{\odot}$ are very long lived. Instead of collapsing into a black hole the bubble radius oscillates between two turning points determined by the net mass. Such oscillating bubbles, rather than supermassive black holes, could be present at galactic centers. Our result can

account for periodic variability observed in near-infrared and X-ray flares from Sagittarius A* [6, 7, 8] and yields the axion mass about 0.6 meV.

Moreover, the bubble scenario with no free parameters (if we fix $m = 0.6$ meV based on Sagittarius A* flare variability) explains lack of supermassive “black holes” with $M < 10^6M_{\odot}$. We find that if $M < 10^6M_{\odot}$ the bubble life time becomes very short, $t \lesssim 10^7$ yrs, and as a result such objects are very rare. We also found that for the exponential metric the bubble mass can not exceed $M_{\text{max}} = 1.5 \times 10^9M_{\odot}$. This, again with no free parameters, explains the upper limit on the supermassive “black hole” mass measured for galactic centers [9].

For axion with mass $m = 0.6$ meV the axion-photon coupling constant is $g_{a\gamma} \sim 10^{-13}\text{GeV}^{-1}$ [29]. Recently it was argued that the solar corona X –ray emission can be explained by solar axions of the Kaluza-Klein type (that is by axions propagating into extra dimensions) which are gravitationally trapped by the Sun and decay near the solar surface [30, 31]. The estimated value of $g_{a\gamma}$ from the analysis of solar corona X –rays is similar to our finding; this is an interesting coincidence.

Observation of the Galactic center with very long-baseline interferometry within the next few years will be capable to test theories of gravitation in the strong field limit. Such an observation will allow us to distinguish between the black hole (predicted by Einstein general relativity) and the oscillating axion bubble scenario which we propose in this paper. If future observations indeed discover periodic appearance of the shadow from the Galactic center object this will also be a strong evidence for the axion nature of dark matter and will lead to an accurate measurement of the axion mass.

I am very grateful to E. Sezgin and N. Suntzeff for useful remarks.

APPENDIX A: DERIVATION OF THE STATIC EXPONENTIAL METRIC FROM THE PRINCIPLE OF SUPERPOSITION

Let us consider a point mass M located at $r = 0$. Static gravitational field produced by the point mass possesses spherical symmetry. Without loss of generality one can look for the metric in an isotropic form

$$ds^2 = -h(r)dt^2 + g(r)(dr^2 + r^2d\theta^2 + r^2\sin^2\theta d\varphi^2). \quad (\text{A1})$$

Einstein equations yield well known Schwarzschild solution [28]

$$h(r) = \left(\frac{1 - M/2r}{1 + M/2r}\right)^2, \quad g(r) = \left(1 + \frac{M}{2r}\right)^4. \quad (\text{A2})$$

Here we derive $h(r)$ and $g(r)$ in a different way. First we note that a static gravitational field of any strength has a potential [28]

$$\phi(r) = \ln \sqrt{h(r)} \quad (\text{A3})$$

and the gravitational force acting on a test rest particle with mass m is

$$\mathbf{f} = -m\nabla\phi \quad \left(f_\alpha = -m\frac{\partial\phi}{\partial x^\alpha} \right). \quad (\text{A4})$$

In Minkowski space-time the potential ϕ satisfies the Poisson equation $\Delta\phi = 4\pi M\delta(\mathbf{r})$. Writing the Laplacian and the delta-function in curvilinear coordinates with metric g_{ik} the Poisson equation yields

$$\frac{1}{\sqrt{-|g_{ik}|}}\frac{\partial}{\partial x^i}\left(\sqrt{-|g_{ik}|}g^{ik}\frac{\partial\phi}{\partial x^k}\right) = \frac{4\pi}{\sqrt{-|g_{ik}|}}M\delta(\mathbf{r}), \quad (\text{A5})$$

where $|g_{ik}|$ is determinant of the metric tensor and g^{ik} is the tensor reciprocal to g_{ik} , that is $g_{ik}g^{kl} = \delta_i^l$. For the metric (A1) Eq. (A5) reduces to

$$\frac{\partial}{\partial r}\left(r^2\sqrt{h(r)g(r)}\frac{\partial\phi(r)}{\partial r}\right) = 4\pi M\delta(r). \quad (\text{A6})$$

Eq. (A6) (with ϕ from Eq. (A3)) describes a relation between the functions h and g which the metric must satisfy. We note that Eq. (A6) is consistent with Einstein general relativity because the Schwarzschild solution (A2) obeys Eq. (A6).

To find the functions h and g we need an additional constraint. Here we postulate that the force of gravity must obey the principle of superposition at any strength of the gravitational field. This is the only difference from Einstein general relativity we introduce. Such way of thoughts makes an appealing connection with the quantum theory.

The principle of superposition is formulated in coordinate systems in which we measure space coordinates by ideal rods unaffected by gravity (e.g. of atomic constitution). This assures that the coordinate system is independent of the position and the value of masses. Let us consider masses M_1 and M_2 located at coordinates \mathbf{r}_1 and \mathbf{r}_2 in the mentioned above coordinate system. The superposition principle means that the gravitational force on any test particle due to masses M_1 and M_2 equals to the vector sum of the force due to the mass M_1 located at \mathbf{r}_1 if there is no mass M_2 and the force due to the mass M_2 located at \mathbf{r}_2 if there is no mass M_1 .

Please note that we formulate the superposition principle for the covariant force vector f_α as in Eq. (A4). This makes a proper connection with the Newtonian limit in which the measurable gravitational force is a covariant vector (under coordinate transformation it transforms like derivatives of a scalar). The covariant force f_α on a test particle is defined as [28] $f_\alpha = md^2x_\alpha/ds^2$, where x_α is the coordinate of the test particle with mass m and ds is the interval. If at the moment when the force is measured the particle has zero velocity (that is when Eq. (A4) applies) then $ds = d\tau$, where τ is the proper time and, hence, $f_\alpha = md^2x_\alpha/d\tau^2$. This equation shows that the definition of the covariant force is unaffected by gravity (if the coordinates x_α are unaffected) and therefore

f_α is the relevant vector to formulate the superposition principle. On the other hand, the contravariant vector $f^\alpha = g^{\alpha\beta}f_\beta$ contains metric in its definition and hence cannot be used in the superposition principle.

It follows from Eqs. (A4) and (A6) that the force of gravity satisfies the principle of superposition if and only if

$$h(r)g(r) = 1, \quad (\text{A7})$$

which yields for arbitrary field strength

$$\frac{\partial}{\partial r}\left(r^2\frac{\partial\phi(r)}{\partial r}\right) = 4\pi M\delta(r). \quad (\text{A8})$$

Hence $\phi(r) = -M/r$ and

$$h(r) = \exp(-2M/r), \quad g(r) = \exp(2M/r). \quad (\text{A9})$$

Eq. (A9) is known as Yilmaz exponential metric [20].

For small M/r both the Schwarzschild (A2) and the exponential (A9) metrics yield the same expansion

$$h(r) = 1 - \frac{2M}{r} + \frac{2M^2}{r^2} + \dots, \quad g(r) = 1 + \frac{2M}{r} + \dots \quad (\text{A10})$$

and hence both metrics pass the four classic weak-field tests of general relativity. Accuracy of current tests is yet far from ability to check the next terms in the expansion (A10) where the two metrics start to deviate from each other [18].

The principle of superposition allows us to find the metric in the case of N point masses M_1, \dots, M_N located at $\mathbf{r}_1, \dots, \mathbf{r}_N$. To apply the principle of superposition we must choose the coordinate system in which we measure space coordinates by ideal rods unaffected by gravity. Since the speed of light measured by such rods and clocks (e.g. of atomic constitution) is independent of direction in a gravitational field the metric in such coordinates is isotropic, that is

$$ds^2 = -h(\mathbf{r})dt^2 + g(\mathbf{r})(dx^2 + dy^2 + dz^2). \quad (\text{A11})$$

For the metric (A11) Eq. (A5) yields

$$\begin{aligned} \frac{\partial}{\partial x}\left(\sqrt{hg}\frac{\partial\phi}{\partial x}\right) + \frac{\partial}{\partial y}\left(\sqrt{hg}\frac{\partial\phi}{\partial y}\right) + \frac{\partial}{\partial z}\left(\sqrt{hg}\frac{\partial\phi}{\partial z}\right) = \\ = 4\pi[M_1\delta(\mathbf{r} - \mathbf{r}_1) + \dots + M_N\delta(\mathbf{r} - \mathbf{r}_N)]. \end{aligned} \quad (\text{A12})$$

The principle of superposition for the potential ϕ (and hence for the force of gravity \mathbf{f}) is satisfied provided $hg = 1$. Then Eqs. (A12) and (A3) give the following answer for N -body space-time geometry in isotropic Cartesian coordinates

$$ds^2 = -e^{2\phi}dt^2 + e^{-2\phi}(dx^2 + dy^2 + dz^2), \quad (\text{A13})$$

where ϕ is the N -body potential

$$\phi(\mathbf{r}) = -\frac{M_1}{|\mathbf{r} - \mathbf{r}_1|} - \dots - \frac{M_N}{|\mathbf{r} - \mathbf{r}_N|}. \quad (\text{A14})$$

Thus, finding the space-time geometry reduces to a simple “electrostatic” problem.

Next we discuss how to obtain the exponential metric from Einstein equations.

1. Derivation of exponential metric from Einstein equations

Einstein equations read

$$R_{ik} - \frac{1}{2}g_{ik}R = 8\pi T_{ik}, \quad (\text{A15})$$

where R_{ik} is the Ricci tensor, R is the scalar space curvature and T_{ik} is the energy-momentum tensor of matter. Let us consider N fixed point masses M_1, \dots, M_N located at $\mathbf{r}_1, \dots, \mathbf{r}_N$. For such a system the energy-momentum tensor in Einstein general relativity is

$$T_0^0 = \sum_{j=1}^N M_j \delta(\mathbf{r} - \mathbf{r}_j), \quad \text{all other } T_i^k = 0. \quad (\text{A16})$$

Solution of Eq. (A15) with this T_{ik} yields black holes and no superposition principle.

To obtain exponential metric we must use another energy-momentum tensor. Let us write T_{ik} by analogy with electrostatic. For N fixed point electric charges q_1, \dots, q_N located at $\mathbf{r}_1, \dots, \mathbf{r}_N$ the energy-momentum tensor is given by [28] (in curvilinear coordinates)

$$T_{ik} = \frac{1}{4\pi} \left(\frac{\partial\phi}{\partial x^i} \frac{\partial\phi}{\partial x^k} - \frac{1}{2}g_{ik}(\nabla\phi)^2 \right), \quad (\text{A17})$$

where $(\nabla\phi)^2 = E_\alpha E^\alpha = g^{\alpha\beta}(\partial\phi/\partial x^\alpha)(\partial\phi/\partial x^\beta)$ and ϕ is the electric potential satisfying the Poisson equation

$$\frac{\partial}{\partial x^i} \left(\sqrt{-|g_{ik}|} g^{ik} \frac{\partial\phi}{\partial x^k} \right) = 4\pi \sum_{j=1}^N q_j \delta(\mathbf{r} - \mathbf{r}_j). \quad (\text{A18})$$

We assume that for the system of N fixed point masses M_1, \dots, M_N the energy-momentum tensor T_{ik} is given by Eqs. (A17) and (A18) with the change $q_j \rightarrow M_j$. Substituting this tensor into Einstein equations (A15) we obtain the solution for the metric given by formulas (A13) and (A14).

One should mention that we can find the proper energy-momentum tensor (A17) simply by plugging the exponential metric (A13) into the left hand side of Einstein equations (A15). Then the “electrostatic” energy-momentum tensor (A17) is obtained automatically.

The result discussed here is valid for a static gravitational field. How to generalize it for time-dependent fields is beyond the scope of the present paper.

APPENDIX B: ENERGY EMISSION FROM A SHRINKING BUBBLE

Here we calculate energy loss by a shrinking spherically symmetric bubble caused by emission of scalar particles (axions). For an order of magnitude estimate one can omit the effect of gravity. Then the evolution of the scalar field $\varphi(t, r)$ is described by sine-Gordon equation

$$\ddot{\varphi} - \varphi'' + \frac{1}{\alpha} \sin(\alpha\varphi) = 2\varphi'/r, \quad (\text{B1})$$

where r is the radial coordinate. Without right-hand side, Eq. (B1) has an exact, so-called kink, solution

$$\varphi_0 = \frac{4}{\alpha} \arctan \left\{ \exp \left[\pm \frac{(r - vt - R_0)}{\sqrt{1 - v^2}} \right] \right\}, \quad (\text{B2})$$

where $R_0 \gg 1$ is the initial bubble radius. The solution describes a kink (space region where φ changes from $2\pi/\alpha$ to 0) propagating with constant velocity v ; the kink’s size is $l \sim \sqrt{1 - v^2}$.

If $l \ll R(t)$, where $R(t)$ is the bubble radius, r.h.s. of (B1) may be treated as a small perturbation. Eq. (B1) possesses approximate solution in the form of the kink (B2) with parameters slowly changing in time under the action of the perturbation. In particular, the kink shrinks due to its surface tension so that the bubble radius and the velocity evolve as [32]

$$R(t) = R_0 \text{cn}(\sqrt{2}t/R_0, 1/\sqrt{2}), \quad v(t) = \sqrt{1 - R^4(t)/R_0^4}, \quad (\text{B3})$$

where cn stands for the elliptic cosine with the modulus $1/\sqrt{2}$. Such a process is accompanied by emission of scalar particles which yields the energy loss. We estimate the energy loss following the original work of Malomed [32, 33]. In terms of the inverse scattering technique, the spectral density of the emitted energy $E_e(t, q)$ is

$$\frac{dE_e}{dq} = \frac{4}{\pi\alpha^2} |B(t, q)|^2, \quad (\text{B4})$$

where q is the radiation wavenumber and the perturbation-induced evolution equation for the complex amplitude $B(t, q)$ is given by [32, 33]

$$\frac{dB}{dt} = -\frac{i}{2(\lambda^2 + \gamma^2)} \int_{-\infty}^{\infty} dr \left(\lambda^2 - \gamma^2 - 2i\lambda\gamma \tanh \left[\frac{r-vt}{\sqrt{1-v^2}} \right] \right) \exp \left(i\sqrt{1+q^2}t - iqr \right) \partial_r \varphi_0, \quad (B5)$$

where $\lambda = \sqrt{1+q^2} - q$ and $\gamma = (1+v)/2\sqrt{1-v^2}$. Calculating the integral in (B5) yields

$$\frac{dB}{dt} = \frac{i\pi [\lambda^2(1-v)(1-\sqrt{1+v}) - v/2]}{(1+v)/4 + \lambda^2(1-v)} \frac{\exp\left(i\sqrt{1+q^2}t - iqvt\right)}{\cosh [\pi q\sqrt{1-v^2}/2]}. \quad (\text{B6})$$

If v slowly varies with time one can take $v \approx \text{const}$ in Eq. (B6), then after integration we obtain

$$B(t, q) = \frac{\pi [\lambda^2(1-v)(1-\sqrt{1+v}) - v/2]}{[(1+v)/4 + \lambda^2(1-v)](\sqrt{1+q^2} - qv)} \frac{\exp(i\sqrt{1+q^2}t - iqv t)}{\cosh[\pi q\sqrt{1-v^2}/2]}. \quad (B7)$$

Therefore

$$\frac{dE_e}{dq} = \frac{16\pi \left[\lambda^2(1-v)(1-\sqrt{1+v}) - v/2 \right]^2}{\alpha^2 \left[(1+v)/4 + \lambda^2(1-v) \right]^2 (\sqrt{1+q^2} - qv)^2} \frac{\sin^2 \left[\left(\sqrt{1+q^2} - qv \right) t/2 \right]}{\cosh^2 \left[\pi q \sqrt{1-v^2}/2 \right]}. \quad (B8)$$

Integration of (B8) over dq gives the emitted energy as a function of time $E_e(t) = \int_{-\infty}^{\infty} dq(dE_e/dq)$. In Eq. (B8) sine is a fast oscillating function, so we substitute $\sin^2(x) \rightarrow 1/2$. The radiation power increases when the kink's velocity v approaches the speed of light $c = 1$. Assuming $1 - v \ll 1$, integration of Eq. (B8) yields

$$E_e(t) \approx \frac{2.51}{\alpha^2(1-v(t))^{3/2}} \approx \frac{7.10}{\alpha^2} \left(\frac{R_0}{R(t)} \right)^6 \quad (B9)$$

The emitted energy becomes comparable with the initial bubble energy $E_0 = 4\pi\sigma R_0^2 = 8R_0^2/\alpha^2$ when the bubble radius reaches the value $R_* \approx R_0^{2/3}$. This value agrees with those obtained in [34].

If the bubble shrinks from the outer turning point R_0 to the inner turning point $R_1 \gg R_*$ the radiated energy is

$$E_e \sim \frac{7.10}{\alpha^2} \left(\frac{R_0}{R_1} \right)^6. \quad (B10)$$

To emit all its energy the bubble must oscillate between R_1 and R_0 about E_0/E_e cycles. As a result, the bubble life-time is

$$t \sim R_0 \frac{E_0}{E_e} \approx \frac{R_1^6}{R_0^3}. \quad (\text{B11})$$

- [1] R.D. Peccei and H.R. Quinn, Phys. Rev. Lett. **38**, 1440 (1977); Phys. Rev. D **16**, 1791 (1977); S. Weinberg, Phys. Rev. Lett. **40**, 223 (1978); F. Wilczek, Phys. Rev. Lett. **40**, 279 (1978).
- [2] R. Bradley, J. Clarke, D. Kinion, L. J. Rosenberg, K. van Bibber, S. Matsuki, M. Mück and P. Sikivie, Rev. Mod. Phys. **75**, 777 (2003).
- [3] G. Raffelt, Space Science Rev. **100**, 153 (2002).
- [4] S. Hannestad, A. Mirizzi and G. Raffelt, J. Cosmol. Astropart. Phys. 07, 002 (2005).
- [5] J.E. Kim, Phys. Rep. **150**, 1 (1987).
- [6] R. Genzel, R. Schödel, T. Ott, A. Eckart, T. Alexander, F. Lacombe, D. Rouan, B. Aschenbach, Nature **425**, 934 (2003).
- [7] S. Gillessen, F. Eisenhauer, E. Quataert, R. Genzel, T. Paumard, S. Trippe, T. Ott, R. Abuter, A. Eckart, P.O. Lagage, M.D. Lehnert, L.J. Tacconi and F. Martins, ApJ **640**, L163 (2006).
- [8] G. Belanger, R. Terrier, O. De Jager, A. Goldwurm and F. Melia, J. Phys.: Conference Series, **54**, 420 (2006).
- [9] A.W. Graham and S.P. Driver, ApJ **655**, 77 (2007).
- [10] H. Falcke, F. Melia, and E. Agol, ApJ **528**, L13 (2000).

[11] H. Falcke, S. Markoff, P.L. Biermann, T.P. Krichbaum, F. Melia, E. Agol, and G. Bower, “Galaxies and their Constituents at the Highest Angular Resolutions”, in Proceedings of IAU Symposium #205, United Kingdom, Edited by R. T. Schilizzi, 2001, p. 28.

[12] Z.Q. Shen, K.Y. Lo, M.C. Liang, P.T.P. Ho and J.H. Zhao, *Nature* **438**, 62 (2005).

[13] L. Huang, M. Shen and F. Yuan, *MNRAS* **379**, 833 (2007).

[14] J. Ipser and P. Sikivie, *Phys. Rev. D* **30**, 712 (1984).

[15] A.A. Svidzinsky, “Intrinsically faint quasars: evidence for meV axion dark matter in the Universe” in Proceedings of the 5th International Conference on Dark Matter in Astro and Particle Physics DARK 2004, College Station, 3-9 October, 2004, Eds. H.V. Klapdor-Kleingrothaus and R. Arnowitt, Springer, p. 523 (2005).

[16] A.A. Svidzinsky, e-print astro-ph/0409064.

[17] M.C. Huang and P. Sikivie, *Phys. Rev. D* **32**, 1560 (1985).

[18] For a recent review see C.M. Will, *Living Rev. Relativity* **9**, 3 (2006).

[19] A generalization of Einstein’s theory which yields the exponential metric in the static limit is a nontrivial problem. One of the possibilities is to include torsion square terms in the Lagrangian [D.B. Chang and H.H. Johnson, *Phys. Rev. D* **21**, 874 (1980); *Phys. Lett. A* **77**, 411 (1980)]. However such a generalization has ghosts [see E. Sezgin and P. van Nieuwenhuizen, *Phys. Rev. D* **21**, 3269 (1980)].

[20] Originally Yilmaz obtained the exponential metric from a scalar field theory [H. Yilmaz, *Phys. Rev.* **111**, 1417 (1958)]. In his second version, Yilmaz obtained the same metric from a tensor-field theory [H. Yilmaz, *Phys. Rev. Lett.* **27**, 1399 (1971)].

[21] H. Yilmaz, *Lett. Nuovo Cimento* **20**, 681 (1977).

[22] This formula can be easily derived using the same line of thoughts as in R.E. Clapp, *Phys. Rev. D* **7**, 345 (1973). For an observer located at the bubble surface the energy is $U_s = 4\pi\sigma R_s^2$, where R_s is the bubble radius in the local frame. To a distant observer a region with the gravitational potential ϕ appears to be compacted by the linear compaction factor e^ϕ , as obtained from (8). The apparent bubble radius R is thus decreased to $R = R_s e^\phi$ which yields a factor $e^{-2\phi}$ if we express U_s in terms of R . A redshift factor e^ϕ reduces the energy for the distant observer to $U = 4\pi\sigma R^2 e^{-\phi}$.

[23] S. K. Blau, E.I. Guendelman and A.H. Guth, *Phys. Rev. D* **35**, 1747 (1987).

[24] A. Aurilia, R. Balbinot and E. Spallucci, *Phys. Lett. B* **262**, 222 (1991).

[25] E. Seidel and W.M. Suen, *Phys. Lett.* **72**, 2516 (1994).

[26] E.W. Kolb and I.I. Tkachev, *Phys. Rev. D* **49**, 5040 (1994).

[27] S.L. Robertson, *ApJ* **515**, 365 (1999).

[28] L.D. Landau and E.M. Lifshitz, *The Classical Theory of Fields* (course of theoretical physics; v.2), Butterworth-Heinemann Ltd, 1995.

[29] G.G. Raffelt, *J. Phys. A: Math. Theor.* **40**, 6607 (2007).

[30] L. DiLella and K. Zioutas, *Astropart. Phys.* **19**, 145 (2003).

[31] K. Zioutas, K. Dennerl, L. DiLella, D.H.H. Hoffmann, J. Jacoby and Th. Papaevangelou, *ApJ.* **607**, 575 (2004).

[32] B.A. Malomed, *Physica* **24D**, 155 (1987).

[33] B.A. Malomed, *Phys. Lett. A* **123**, 459 (1987).

[34] L.M. Widrow, *Phys. Rev. D* **40**, 1002 (1989).